UCRL-JRNL-213850

LAWRENCE
LIVERMORE
NATIONAL
LABORATORY

Shape transitions in neutron-rich Ru isotopes: spectroscopy of ^{109,110,111,112}Ru

C.Y. Wu
Lawrence Livermore National Laboratory, Livermore, CA 94551
H. Hua, D. Cline, A.B. Hayes, R. Teng, and D. Riley
NSRL, University of Rochester, Rochester, NY 14627
R.M. Clark, P. Fallon, A. Goergen, A.O. Macchiavelli, and K. vetter
Nuclear Science Division, Lawrence Berkeley National Laboratory, Berkeley, CA 94720

July 22, 2005

Preprint of paper submitted to Physical Review C

Shape transitions in neutron-rich Ru isotopes: spectroscopy of ^{109,110,111,112}Ru

C.Y. Wu
Lawrence Livermore National Laboratory, Livermore, CA 94551

H. Hua, D. Cline, A.B. Hayes, R. Teng, and D. Riley
Nuclear Structure Research Laboratory, Department of Physics, University of Rochester, Rochester, NY 14627

R.M. Clark, P. Fallon, A. Goergen, A.O. Macchiavelli, and K. Vetter
Nuclear Science Division, Lawrence Berkeley National Laboratory, Berkeley, CA 94720

Abstract

The spectroscopy of neutron-rich ^{109,110,111,112}Ru nuclei was studied by measuring the prompt γ rays originated from fission fragments, produced by the ^{238}U(α,*f*) fusion-fission reaction, in coincidence with the detection of both fragments. For ^{109,111}Ru, both the negative-parity ($h_{11/2}$ orbitals) and positive-parity ($g_{7/2}$ and/or $d_{5/2}$ orbitals) bands were extended to substantially higher spin and excitation energy than known previously. The ground-state and γ-vibrational bands of ^{110,112}Ru also were extended to higher spin, allowing observation of the second band crossing at the rotational frequency of ≈450 keV in ^{112}Ru, which is ≈50 keV above the first band crossing. At a similar rotational frequency, the first band crossing for the $h_{11/2}$ band in ^{111}Ru was observed, which is absent in ^{109}Ru. These band crossings most likely are caused by the alignment of the $g_{9/2}$ proton pair. This early onset of the band crossing for the aligned $\pi g_{9/2}$ orbitals may be evidence of a triaxial shape transition from prolate to oblate occurring in ^{111}Ru. The data together with a comparison of cranked shell model predictions are presented.

PACS numbers: 23.20.Lv,25.70.Jj,27.60.+j

Keyword: NUCLEAR STRUCTURE ^{109,110,111,112}Ru; populated by the ^{238}U(α,f) fusion-fission reaction, rotational and vibrational structure, measured $B(M1)/B(E2)$ ratios, rotational bands built on the $d_{5/2}$, $g_{7/2}$, and $h_{11/2}$ neutron orbitals.

I. Introduction

For neutron-rich A≥100 nuclei, the nuclear shape changes very rapidly as the valence nucleons fill the $g_{9/2}$ proton and $h_{11/2}$ neutron orbitals, which is manifest by such phenomena as the sudden onset of quadrupole deformation in Sr-Zr isotopes, the development of triaxial degrees of freedom in Mo-Ru isotopes, and the predicted transition of a triaxial shape from prolate to oblate in Ru-Pd isotopes. The ramifications on the nuclear structure due to various shapes make these neutron-rich nuclei an ideal testing ground for various theoretical models [1-3]. For instance, the exact location where shape transitions occur is very sensitive to the model assumptions. A prolate to oblate shape transition for Pd isotopes is predicted to happen at ^{111}Pd by the finite-range droplet model (FRDM) [1] and at ^{112}Pd by the relativistic mean-field (RMF) theory [3]. Both calculations were made for nuclei across the period table but the latter was only applied to even-even nuclei. Calculations using the Nilsson-Strutinsky method with the cranked Woods-Saxon average potential and a monopole pairing residual interaction [2], which were applied to even-even neutron-rich A≈100 nuclei, predict the transition occurring at ^{116}Pd. Experimental verification of this shape transition has important implications on our understanding of the residual interactions in neutron-rich nuclei. In this paper, we discuss the experimental evidence for a prolate-to-oblate shape transition in neutron-rich Ru isotopes resulting from the study of the γ-ray spectroscopy of fission fragments. The preliminary results of this shape transition in Ru-Pd isotopes have been presented in our earlier publications [4,5].

To distinguish a prolate from an oblate quadrupole deformation, one needs to measure the sign of the static quadrupole moment for the state of interest. Typically, this can be accomplished using the Coulomb excitation technique. For example, a prolate-to-oblate shape transition was identified in ^{192}Os-^{194}Pt isotones by measuring both the magnitude and sign of static quadrupole moments for their first 2^+ states using Coulomb excitation [6-8]. This shape transition was predicted by Kumar and Baranger from solving Bohr's Hamiltonian using the pairing-plus-quadrupole model [9-11]. However, this experimental technique is difficult to apply for nuclei away from the valley of β stability such as neutron-rich Ru-Pd isotopes. An alternative approach is to recognize processes that may yield a distinct signature to differentiate between two shapes. In this work, we explore one such opportunity to address evidence of a triaxial shape transition from prolate to oblate in neutron-rich Ru isotopes by studying the band crossing phenomenon, which is sensitive to the interplay between the single-particle and shape degrees of freedom.

II. Experiment

The neutron-rich Ru isotopes were produced as fission fragments by the ^{238}U(α,*f*) fusion-fission reaction. The experiment was carried out at the 88-inch cyclotron facility of the Lawrence Berkeley National Laboratory by bombarding a ≈300 μg/cm^2 ^{238}U target on a ≈30 μg/cm^2 carbon backing with an α beam at E_{lab}=30 MeV. Fission fragments were detected by the Rochester 4π, highly-segmented heavy-ion detector array, CHICO [12,13], in coincidence with the detection of deexcitation γ rays using Gammasphere. This particle detector has a geometric coverage for scattering angles from 12^o to 85^o and 95^o to 168^o relative to the beam axis and an azimuthal angle totaling 280^o out of 360^o. A valid event required the detection of both fission fragments and at least three coincident γ rays. Scattering angles of fission fragments and the time-of-flight difference

between two fragments were recorded in addition to the γ-ray energies and coincident time. A total of ≈6×10^8 p-p-γ-γ-γ five-fold coincident events were collected.

From the measured fission kinematics, one can deduce masses and velocity vectors of both fragments assuming the total kinetic energy is the same as that for ^{240}Pu spontaneous fission [14]. This assumption, that the prompt fission originates from a Pu-like compound nucleus, was supported by the cross correlation between the observed γ rays from partner fragment pairs. The deduced mass spectrum of fission fragments has a resolution about 12 mass units, which reflects a time resolution of ≈500 ps in addition to the position resolution of ≈1^o in polar angle and 4.6^o in azimuthal angle. The achieved resolutions are consistent with prior CHICO performance [15-21].

Three or higher coincident γ rays with mass-gated events were used to develop the level schemes of ^{109,110,111,112}Ru. The added selectivity, given by the mass gate, reduces the "background" γ rays of nuclei that are not of current interest, which enhances the ability to study nuclei produced with low yield or having weak transition strengths. Doppler-shift corrected γ-ray spectra, gated by the mass and known γ-ray transitions in ^{109}Ru and ^{111}Ru, are shown in Fig. 1. The achieved energy resolution is better than 1%, limited primarily by the finite size of Ge detector. Since the origin of γ rays from either fission fragment was established after the proper Doppler-shift corrections were made, the γ-ray transitions from partner fragments are Doppler broadened making them not visible in these spectra. The resultant spectra are clean and straightforward to interpret.

III. Results and discussion

A. ^{109}Ru and ^{111}Ru

Comprehensive information on the spectroscopy of ^{109,111}Ru was achieved only recently by experiments measuring high-fold γ-ray transitions for fission fragments produced by either ^{248}Cm or ^{252}Cf sealed fission sources [22-24]. Further expansion of the level schemes of these nuclei to even higher angular momentum and excitation energy was achieved in the present work. The $K^\pi=5/2^+$ band was extended from $19/2^+$ and $23/2^+$ to $33/2^+$ at 4750.4 keV and $35/2^+$ at 5168.4 keV for ^{109}Ru and ^{111}Ru, respectively. The assignment for the $21/2^+$ state at 2274.0 keV in ^{109}Ru [22] was not confirmed by the present work. The $K^\pi=5/2^-$ band in ^{109}Ru was extended from $27/2^-$ to $39/2^-$ at 5804.1 keV while the $K^\pi=7/2^-$ band in ^{111}Ru was extended from $31/2^-$ to $47/2^-$ at 7498.2 keV. Level schemes derived from this work are shown in Figs. 2 and 3 for ^{109}Ru and ^{111}Ru, respectively.

For the negative-parity bands of ^{109,111}Ru, the odd neutron most probably occupies the subshell of $h_{11/2}$ orbitals as has been discussed in detail in Ref. [23,24]. The moments of inertia versus rotational frequency are shown in Figs. 4 and 5 for ^{109}Ru and ^{111}Ru, respectively. They are very similar for the two isotopes until the rotational frequency increases to above ≈450 keV, where a sudden upbend is observed for ^{111}Ru but not for ^{109}Ru. Note that the band crossing phenomenon in the neutron-rich A≥100 nuclei is mainly caused by the alignment of either the $\nu h_{11/2}$ or $\pi g_{9/2}$ orbitals. The blocking effect plus the non-observation of band crossing in ^{109}Ru eliminates the possibility of the $\nu h_{11/2}$ orbitals being responsible for the observed upbend in ^{111}Ru. The crossing frequency is more sensitive to triaxial degrees of freedom for the $\pi g_{9/2}$ orbitals compared to the $\nu h_{11/2}$ orbitals [2]. Therefore, the observed disparity in the moment-of-inertia plot may be related to

a triaxial shape transition from prolate to oblate between ^{109}Ru and ^{111}Ru, which causes an early onset of the band crossing for the alignment of a pair $g_{9/2}$ proton in ^{111}Ru.

For the positive-parity $K^{\pi}=5/2^{+}$ band in ^{111}Ru, the authors in Ref. [24] argue that the dominant component of the underlying single-particle configuration is the $5/2^{+}[402]$ subshell, originating from the $g_{7/2}$, for states below $15/2^{+}$ and changes to the $5/2^{+}[413]$ subshell of the $d_{5/2}$ origin, for states above $15/2^{+}$ in order to explain the signature inversion observed for the ΔI=1 energy splitting between the two signatures. However, the same phenomenon observed in ^{107}Ru was interpreted as being due to triaxiality [25]. One striking observation in our study of the $K^{\pi}=5/2^{+}$ band is the large amplitude of the energy splitting seen in ^{109}Ru disappears in ^{111}Ru for rotational frequencies above 400 keV as shown in Figs. 4 and 5, where a band crossing due to the aligned $\nu h_{11/2}$ orbitals is possible. Note that the amplitude of energy splitting is a measure of the Ω=1/2 component in the wavefunction. Our observation implies that the Ω=1/2 subshell is occupied in ^{109}Ru but not in ^{111}Ru. One possible scenario for this happening is a shape transition from prolate to oblate between ^{109}Ru and ^{111}Ru, resulting in the arrangement of Ω subshells being reversed.

The underlying single-particle configuration also can be probed by the magnetic properties of these rotational bands, such as the $B(M1)/B(E2)$ ratios. They can be derived experimentally from the γ-ray intensity ratios of the $\Delta I=1$ to $\Delta I=2$ transitions and can be calculated for any given single-particle configuration under the assumption of a rotor. A number of these relative γ-decay branching ratios for members of both negative and positive-parity bands in ^{109}Ru and ^{111}Ru were measured in this work and are listed in Table I together with the values from other work. The agreement with earlier measurements is about a factor of 2; the reason for this poor agreement is not clear. However, the current measurements should be less likely to suffer from interferences of the many competing fission products because they were derived from the spectra gated by the feeding transitions.

The derived $B(M1)/B(E2)$ ratios together with the calculated ones for various subshells for both negative and positive-parity bands in ^{109,111}Ru are listed in Table II. A rotor is assumed for the model calculation with the g_K derived from Ref. [27], $g_R=0.5Z/A\approx0.2$ [28], and $Q_0=3.31$ eb (adapted from the neighboring even-even Ru isotopes [29]) for either a pure prolate ($\gamma=0^{o}$) or a pure oblate ($\gamma=-60^{o}$) shape. No unambiguous statement can be made for the underlying single-particle configuration of those rotational bands by the comparison between the data and model calculations. However, a strong mixing between $5/2^{+}[413]$, of $d_{5/2}$ origin, and $5/2^{+}[402]$, of $g_{7/2}$ origin, is suggested to explain the experimental data for the positive-parity bands. For the negative-parity bands, the results may not be a surprise since configuration mixing for the $h_{11/2}$ orbitals is expected due to the Coriolis interaction.

B. ^{110}Ru and ^{112}Ru

The high-spin structure of ^{110,112}Ru has been studied extensively using the γ-ray spectroscopy of fission fragments produced by either ^{248}Cm or ^{252}Cf sources in a sealed or open form [12,30-34]. In the present work, the ground-state bands were extended to spin 22^{+} at 8161.1 and 7751.4 keV for ^{110}Ru and ^{112}Ru, respectively. The γ-vibrational bands were extended to spin 15^{+} at 5542.6 keV in

^{110}Ru and to spin 19^+ at 6799.9 keV in ^{112}Ru. The deduced level schemes are shown in Fig. 6 and 7 for ^{110}Ru and ^{112}Ru, respectively.

As discussed in our earlier publications [4,5] and others [31,33], the first band crossing occurring at a rotational frequency ≈400 keV was observed for ^{110}Ru as well as ^{112}Ru and most likely is attributed to the aligned $\nu h_{11/2}$ orbitals. A surprising observation from this work, by extending the level schemes to higher angular momentum and excitation energy, is the second band crossing occurring at the rotational frequency ≈450 keV in ^{112}Ru but not in ^{110}Ru as shown in Figs. 8 and 9, where the moments of inertia vs. rotational frequency are plotted for ^{110}Ru and ^{112}Ru, respectively. Note that this band crossing happens at nearly identical frequency to that of the $\nu h_{11/2}$ band in ^{111}Ru and may also be related to the aligned $\pi g_{9/2}$ orbitals in a triaxial shape with an oblate deformation.

To understand this complex band crossing phenomena in the framework of the cranked shell model [35], we performed calculations using a Woods-Saxon potential with the quadrupole deformation β_2=0.29 [29] and γ=−26^o or −34^o for both quasineutrons and quasiprotons in ^{112}Ru. The results are shown in Figs. 10 and 11. The predicted crossing frequency for the aligned $\nu h_{11/2}$ orbitals is relatively insensitive to a prolate-to-oblate shape change but is ≈100 keV lower than the observed value, shown in Fig. 10. As the triaxial shape changes from prolate to oblate, a well-localized crossing, which is about 50 keV higher than the observed value, is predicted for the aligned $\pi g_{9/2}$ orbitals as shown in Fig. 11. The cranked shell model description explains qualitatively the observed band crossing phenomena in these Ru isotopes.

A 10^+ band, with excitation energy at 3192.7 keV, was tentatively identified up to spin 18^+ at 6018.0 keV in ^{110}Ru [33]. The bandhead feeds the 8^+ and 9^+ states of the γ-vibrational band and could be interpreted as the yrast 10^+ state with a crossing frequency similar to that of the ground-state band. However, it was not observed in this experiment. The continuation of the γ-vibrational band was extended to spin 15^+ at 5542.6 keV in ^{110}Ru and to spin 19^+ at 6799.9 keV in ^{112}Ru from the current work. In the earlier studies [30,31] of even-even neutron-rich Ru isotopes, the electromagnetic properties of the γ-vibrational bands are well described by a rigid triaxial rotor for lower-spin states and by the rotation-vibration collective model for the higher-spin states. This interpretation may be fortuitously supported by the observation of nearly identical moments of inertia, for rotational frequency below the first band crossing, between the ground-state and the γ-vibrational bands for both ^{110}Ru and ^{112}Ru, which are illustrated in Figs. 8 and 9, respectively. The consequence of a weak pairing is the more likely explanation for this observation. Further experimental and theoretical works are needed to understand these intriguing phenomena.

IV. Summary

The spectroscopy study of neutron-rich ^{109,110,111,112}Ru has been carried out using the prompt γ rays emitted from fission fragments, produced by the ^{238}U(α,*f*) fusion-fission reaction. Level schemes were extended to much higher angular momentum and excitation energy than previously known, especially for ^{109}Ru and ^{111}Ru, due to the much greater selectivity and sensitivity of the γ-fission-fragment coincident technique. This extension allowed observation of a complex band crossing phenomenon in these neutron-rich Ru isotopes. A lower crossing frequency for the aligned $\pi g_{9/2}$ orbitals is the most likely reason for the second band crossing observed in ^{112}Ru as well as the band

crossing observed for the $\nu h_{11/2}$ band in ^{111}Ru. The occupancy level of the Ω=1/2 subshell may explain a significant difference of the energy splitting for the positive-parity band at rotational frequencies above 400 keV, between ^{109}Ru and ^{111}Ru. All these can be interpreted consistently as a triaxial shape transition from prolate to oblate occurring in ^{111}Ru. This complex band crossing phenomenon also is elucidated qualitatively by the cranked shell model calculations. Further study is needed to understand the electromagnetic properties of the γ-vibrational bands in ^{110}Ru and ^{112}Ru, which have many characteristics of a triaxial rigid rotor even though they are believed to be γ-soft nuclei.

Acknowledgments

This work was performed in part under the auspices of the U.S. Department of Energy by the University of California, Lawrence Livermore National Laboratory under contracts no. W-7405-ENG-48. The work by the Rochester group was funded by NSF and AFOSR. The work at LBNL was supported in part by the U.S. DoE under contract No. DE--AC03--76SF00098.

References

[1] P. Moller, J.R. Nix, W.D. Myers, and W.J. Swiatecki, At. Data Nucl. Data Tables **59**, 185 (1995).
[2] J. Skalski, S. Mizutori, and W. Nazarewicz, Nucl. Phys. A **617**, 282 (1997).
[3] G.A. Lalazissis, S. Raman, and P. Ring, At. Data Nucl. Data Tables **71**, 1 (1999).
[4] C.Y. Wu, H. Hua, D. Cline, A.B. Hayes, R. Teng, R.M. Clark, P. Fallon, A. Goergen, A.O. Macchiavelli, and K. Vetter, *Proceedings of the Third International Conference on Fission and Properties of Neutron-Rich Nuclei, Sanibel Island, FL,* edited by J.H. Hamilton, A.V. Ramayya, and H.K. Carter (World Scientific, Singapore, 2003), p. 199.
[5] H. Hua, C.Y. Wu, D. Cline, A.B. Hayes, R. Teng, R.M. Clark, P. Fallon, A. Goergen, A.O. Macchiavelli, and K. Vetter, Phys. Lett. B **562**, 201 (2003).
[6] J.E. Glenn and J.X. Saladin, Phys. Rev. Lett. **20**, 1298 (1968).
[7] R.J. Pryor and J.X. Saladin, Phys. Rev. C **4**, 1573 (1970).
[8] C.Y. Wu *et al*., Nucl. Phys. **A 607**, 178 (1996).
[9] K. Kumar and M. Baranger, Phys. Rev. Lett. **17**, 1146 (1966).
[10] K. Kumar and M. Baranger, Nucl. Phys. **A 122**, 273 (1968).
[11] K. Kumar, Phys. Rev. C **1**, 369 (1970).
[12] M.W. Simon, Ph.D. thesis, University of Rochester, 1999.
[13] M.W. Simon, D. Cline, C.Y. Wu, R.W. Gray, R. Teng, and C. Long, Nucl. Instrum. Methods Phys. Res. A **452**, 205 (2000).
[14] J. Weber, H. Specht, E. Konechy, and D. Heunemann, Nucl. Phys. A **221**, 414 (1974).
[15] K. Vetter *et al*., Phys. Rev. C **58**, 2631 (1998).
[16] C.Y. Wu, M.W. Simon, D. Cline, G.A. Davis, R. Teng, A.O. Macchiavelli, and K. Vetter, Phys. Rev. C **64**, 064317 (2001).
[17] A.B. Hayes *et al*., Phys. Rev. Lett. **89**, 242501 (2002).
[18] A.B. Hayes, Ph.D. thesis, University of Rochester, 2005.
[19] C.Y. Wu, D. Cline, M.W. Simon, R. Teng, K. Vetter, M.P. Carpenter, R.V.F. Janssens, and I. Wiedenhover, Phys. Rev. C **68**, 044305 (2003).
[20] P.H. Regan *et. al*., Phys. Rev. C **68**, 044313 (2003).
[21] J.J. Valiente-Dobon *et al*., Phys. Rev. C **69**, 024316 (2004).
[22] K. Butler-Moore *et al*., Phys. Rev. C **52**, 1339 (1995).
[23] J.K. Hwang *et al*., J. Phys. G: Nucl. Part. Phys. **24**, L9 (1998).
[24] W. Urban *et al*., Eur. Phys. J. A **22**, 231 (2004).
[25] S.J. Zhu et al., Phys. Rev. C **65**, 014307 (2002).
[26] J. Blachot, Nucl. Data sheets **86**, 505 (1999).
[27] E. Browne and F.R. Femenia, Nucl. Data Tables **10**, 81 (1971).
[28] H. Mach, F.K. Wohn, M. Moszynski, R.L. Gill, and R.F. Casten, Phys. Rev. C **41**, 1141 (1990).
[29] S. Raman, C.H. Malarkey, W.T. Milner, C.W. Nestor, Jr., and P.H. Stelson, At. Data Nucl. Data Tables **36**, 1 (1987).
[30] J.A. Shannon *et al*., Phys. Lett. B **336**, 136 (1994).
[31] Q.H. Lu *et al*., Phys. Rev. C **52**, 1348 (1995).
[32] M.W. Simon *et al*., *Proceedings of the International Conference on Fission and Properties of Neutron Rich Nuclei, Sanibel Island, FL,* edited by J.H. Hamilton and A.V. Ramayya, (World Scientific, Singapore, 1998), p. 270.

[33] Z. Jiang *et al*., Chin. Phys. Lett. **20**, 350 (2003).
[34] S.J. Zhu *et al*., *Proceedings of the Third International Conference on Fission and Properties of Neutron-Rich Nuclei, Sanibel Island, FL,* edited by J.H. Hamilton, A.V. Ramayya, and H.K. Carter (World Scientific, Singapore, 2003), p. 191.
[35] R. Wyss, lecture delivered at the *Hands on Nuclear Structure Theory Workshop*, Oak Ridge, Tennessee, 1991 (unpublished).

Figure captions

Figure 1. Doppler-shift corrected prompt γ-ray spectrum derived from multiple double-gates placed on prompt transitions of the positive-parity ($g_{7/2}$ and/or $d_{5/2}$ orbitals) band in ^{109}Ru (top) and the negative-parity ($h_{11/2}$ orbitals) band in ^{111}Ru (bottom).

Figure 2. Partial level scheme of ^{109}Ru with energies labeled in keV. The uncertainty on the transition energies is ≈1 keV.

Figure 3. Partial level scheme of ^{111}Ru with energies labeled in keV. The uncertainty on the transition energies is ≈1 keV.

Figure 4. Kinematic moment of inertia as a function of rotational frequency for both positive and negative-parity bands in ^{109}Ru.

Figure 5. Kinematic moment of inertia as a function of rotational frequency for both positive and negative-parity bands in ^{111}Ru.

Figure 6. Partial level scheme of ^{110}Ru with energies labeled in keV. The uncertainty on the transition energies is ≈1 keV.

Figure 7. Partial level scheme of ^{112}Ru with energies labeled in keV. The uncertainty on the transition energies is ≈1 keV.

Figure 8. Kinematic moment of inertia as a function of rotational frequency for both ground-state band, labeled by filled circles, and γ-vibrational band, labeled by filled and open squares, in ^{110}Ru.

Figure 9. Kinematic moment of inertia as a function of rotational frequency for both ground-state band, labeled by filled circles, and γ-vibrational band, labeled by filled and open squares, in ^{112}Ru.

Figure 10. Cranked shell model calculations for quasineutrons in ^{112}Ru with β_2=0.29, β_4=0.0, and γ=−26^o (top) and −34^o (bottom). (π,α): solid=(+,+1/2), dotted=(+,−1/2), dash-dotted=(−,+1/2), dashed=(−,−1/2).

Figure 11. Cranked shell model calculations for quasiprotons in ^{112}Ru with β_2=0.29, β_4=0.0, and γ=−26^o (top) and −34^o (bottom). (π,α): solid=(+,+1/2), dotted=(+,−1/2), dash-dotted=(−,+1/2), dashed=(−,−1/2).

Table I. Relative γ-ray intensities for transitions in ^{109}Ru and ^{111}Ru. The statistic error is quoted for the measured relative intensity in this work and the systematic error could be up to 30% for the weak branches.

Transition	E_γ (keV)	Relative intensity	
		This work	Other work[a]
	^{109}Ru		
$13/2^- \rightarrow 9/2^-$	389.1	1.00	1.00
$\rightarrow 11/2^-$	313.9	0.74(8)	1.61
$17/2^- \rightarrow 13/2^-$	565.1	1.00	1.00
$\rightarrow 15/2^-$	504.7	0.66(10)	0.54
$9/2^+ \rightarrow 5/2^+$	407.8	1.00	1.00
$\rightarrow 7/2^+$	222.7	0.72(6)	0.34
$11/2^+ \rightarrow 7/2^+$	472.5	1.00	1.00
$\rightarrow 9/2^+$	249.8	0.31(9)	0.55
$13/2^+ \rightarrow 9/2^+$	540.6	1.00	1.00
$\rightarrow 11/2^+$	290.8	0.14(1.3)	0.41
	^{111}Ru		
$13/2^- \rightarrow 9/2^-$	378.6	1.00	1.00
$\rightarrow 11/2^-$	302.7	0.73(7)	0.95(5)
$17/2^- \rightarrow 13/2^-$	532.2	1.00	1.00
$\rightarrow 15/2^-$	477.9	0.93(9)	0.52(6)
$9/2^+ \rightarrow 5/2^+$	355.9	1.00	1.00
$\rightarrow 7/2^+$	205.7	0.88(10)	0.54(7)
$11/2^+ \rightarrow 7/2^+$	431.4	1.00	1.00
$\rightarrow 9/2^+$	225.7	0.29(4)	0.19(4)

[a] The data for ^{109}Ru and ^{111}Ru are from Ref. [26] and Ref. [24], respectively.

Table II. Comparison of the $B(M1)/B(E2)$ ratio between the experimental values derived from the present work and the calculated ones using the rotational model with the single-particle configurations specified for both positive and negative states in ^{109}Ru and ^{111}Ru. Pure $M1$ was assumed for the $\Delta I=1$ transitions. The model values for $B(M1)/B(E2)$ ratios listed in the first row are calculated assuming a prolate shape and the values for an oblate shape are listed in the second row.

Initial state	B(M1)/B(E2) (μ_N^2/e^2b^2)					
	Experiment		Calculation			
	^{109}Ru	^{111}Ru				
			Configuration			
			$1/2^-[550]$	$3/2^-[541]$	$5/2^-[532]$	$7/2^-[523]$
$13/2^-$	0.148(15)	0.143(13)	0.073	0.308	0.695	1.45
			0.00053	0.170	0.226	1.21
$17/2^-$	0.207(31)	0.254(24)	0.071	0.290	0.607	1.08
			0.00051	0.160	0.197	0.91
			Configuration			
			$5/2^+[413]$	$5/2^+[402]$		
$9/2^+$	0.511(44)	0.403(44)	0.109	1.80		
			0.134	0.73		
$11/2^+$	0.329(29)	0.267(33)	0.075	1.24		
			0.092	0.51		
$13/2^+$	0.188(17)		0.064	1.05		
			0.079	0.43		

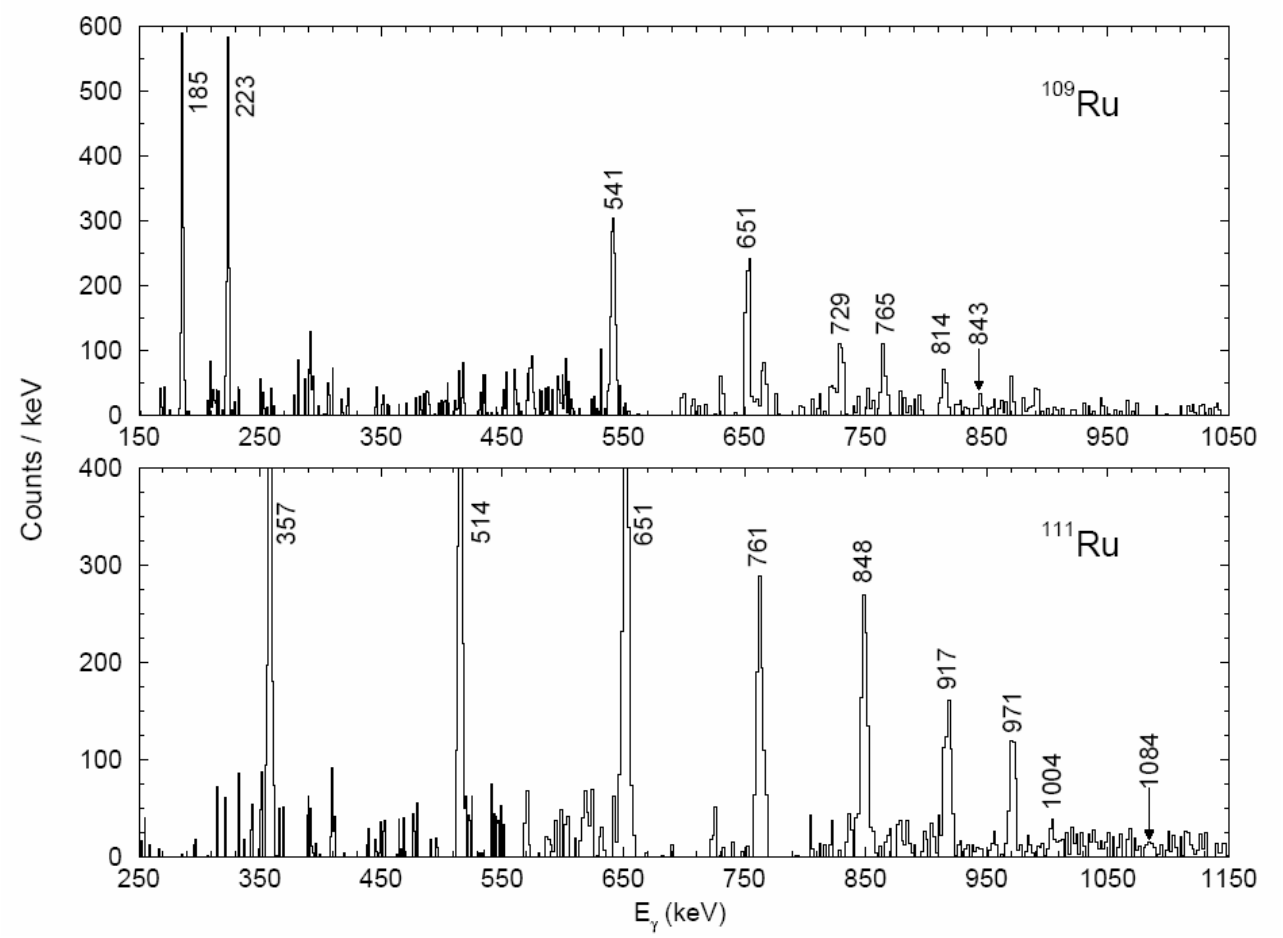

Figure 1. Doppler-shift corrected prompt γ-ray spectrum derived from multiple double-gates placed on prompt transitions of the positive-parity ($g_{7/2}$ and/or $d_{5/2}$ orbitals) band in ^{109}Ru (top) and the negative-parity ($h_{11/2}$ orbitals) band in ^{111}Ru (bottom).

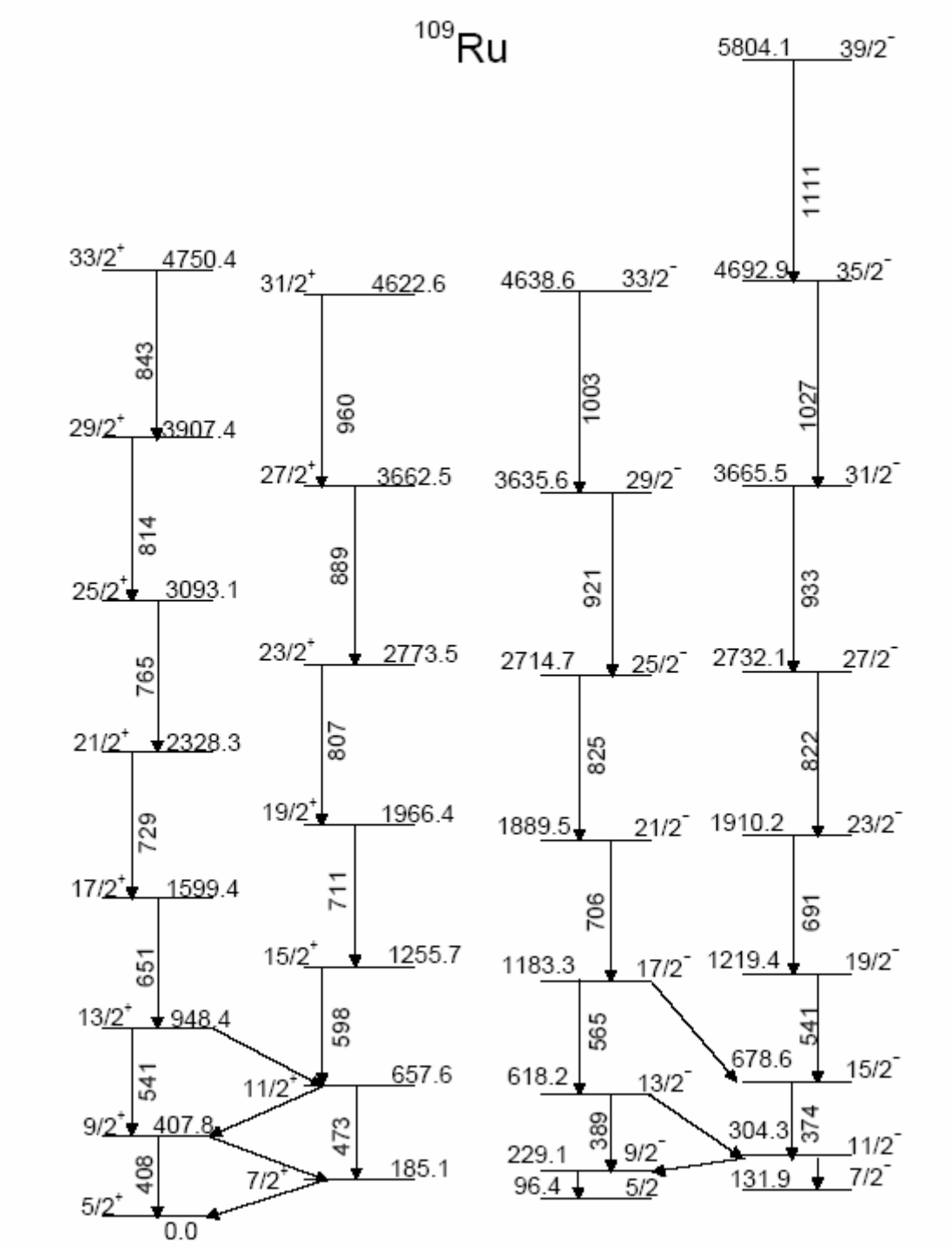

Figure 2. Partial level scheme of ^{109}Ru with energies labeled in keV. The uncertainty on the transition energies is ≈1 keV.

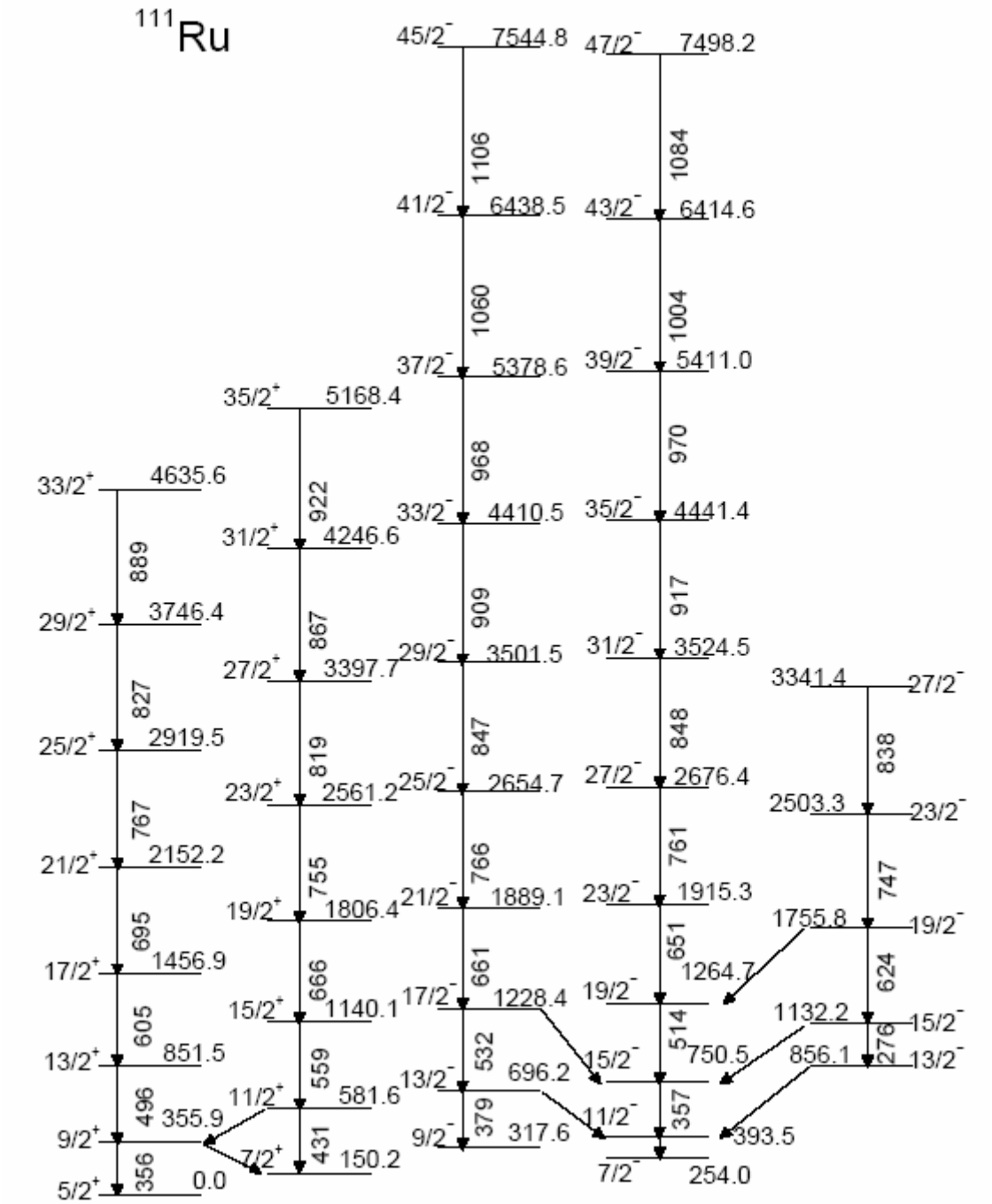

Figure 3. Partial level scheme of ^{111}Ru with energies labeled in keV. The uncertainty on the transition energies is ≈1 keV.

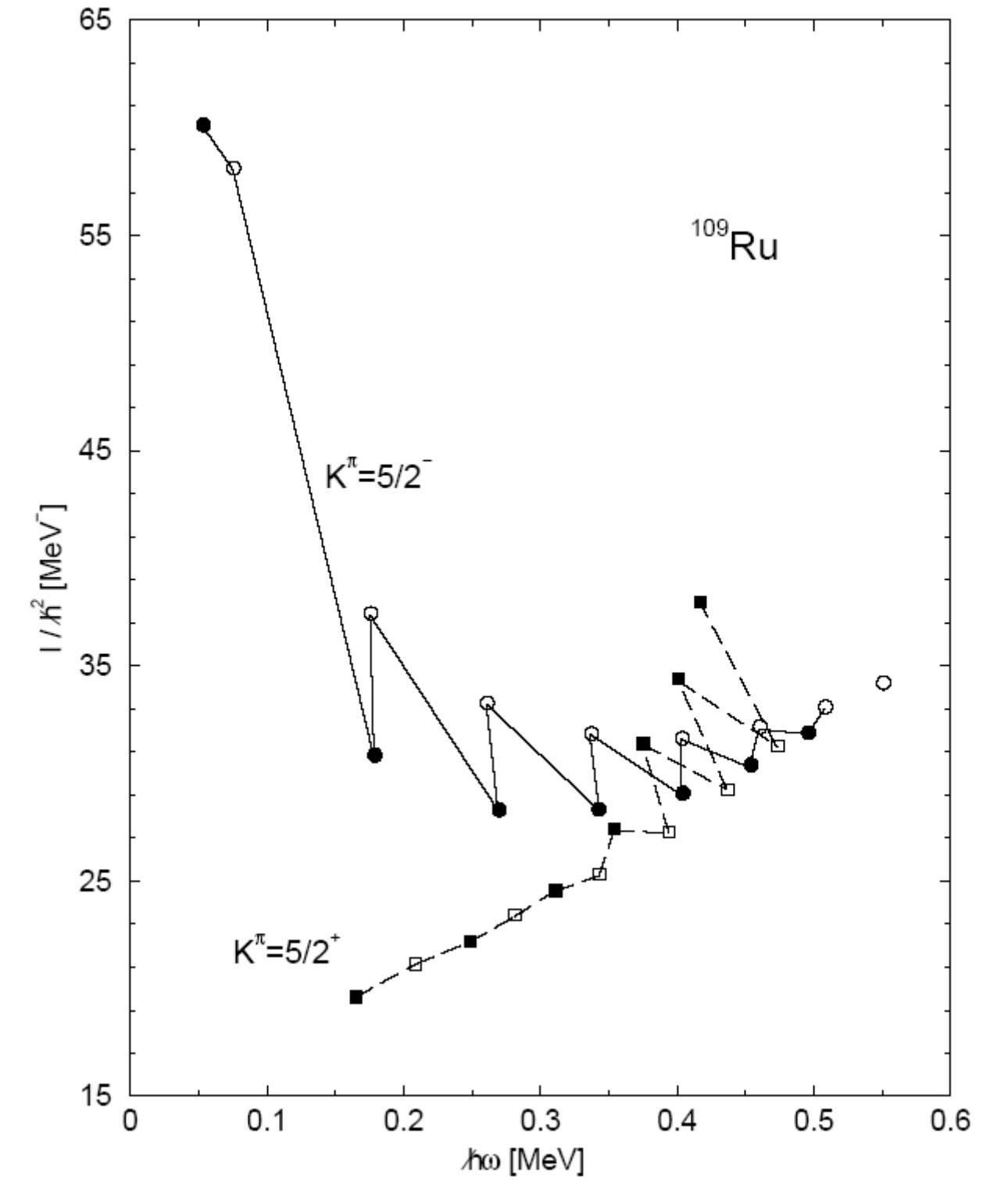

Figure 4. Kinematic moment of inertia as a function of rotational frequency for both positive and negative-parity bands in ^{109}Ru.

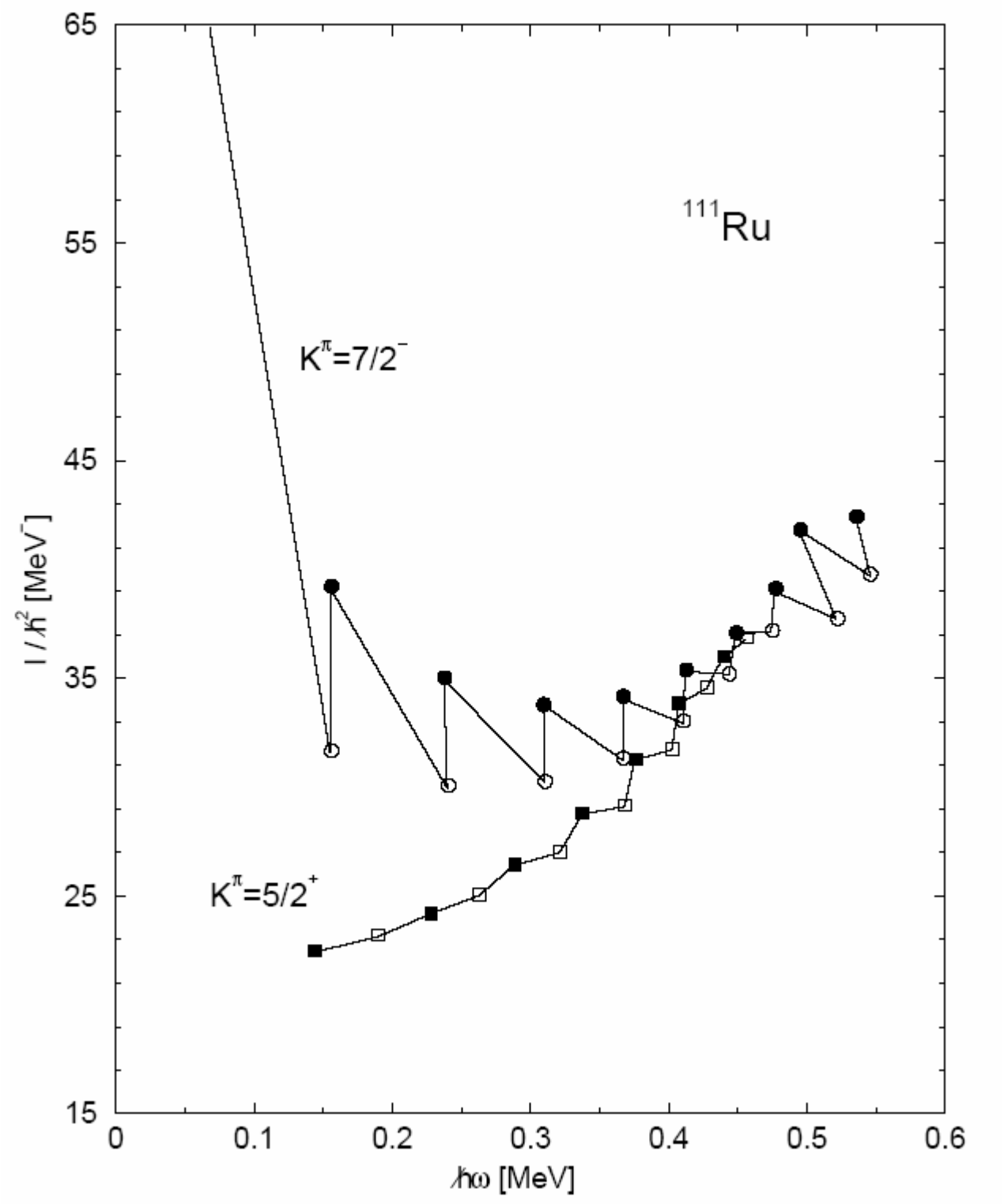

Figure 5. Kinematic moment of inertia as a function of rotational frequency for both positive and negative-parity bands in ^{111}Ru.

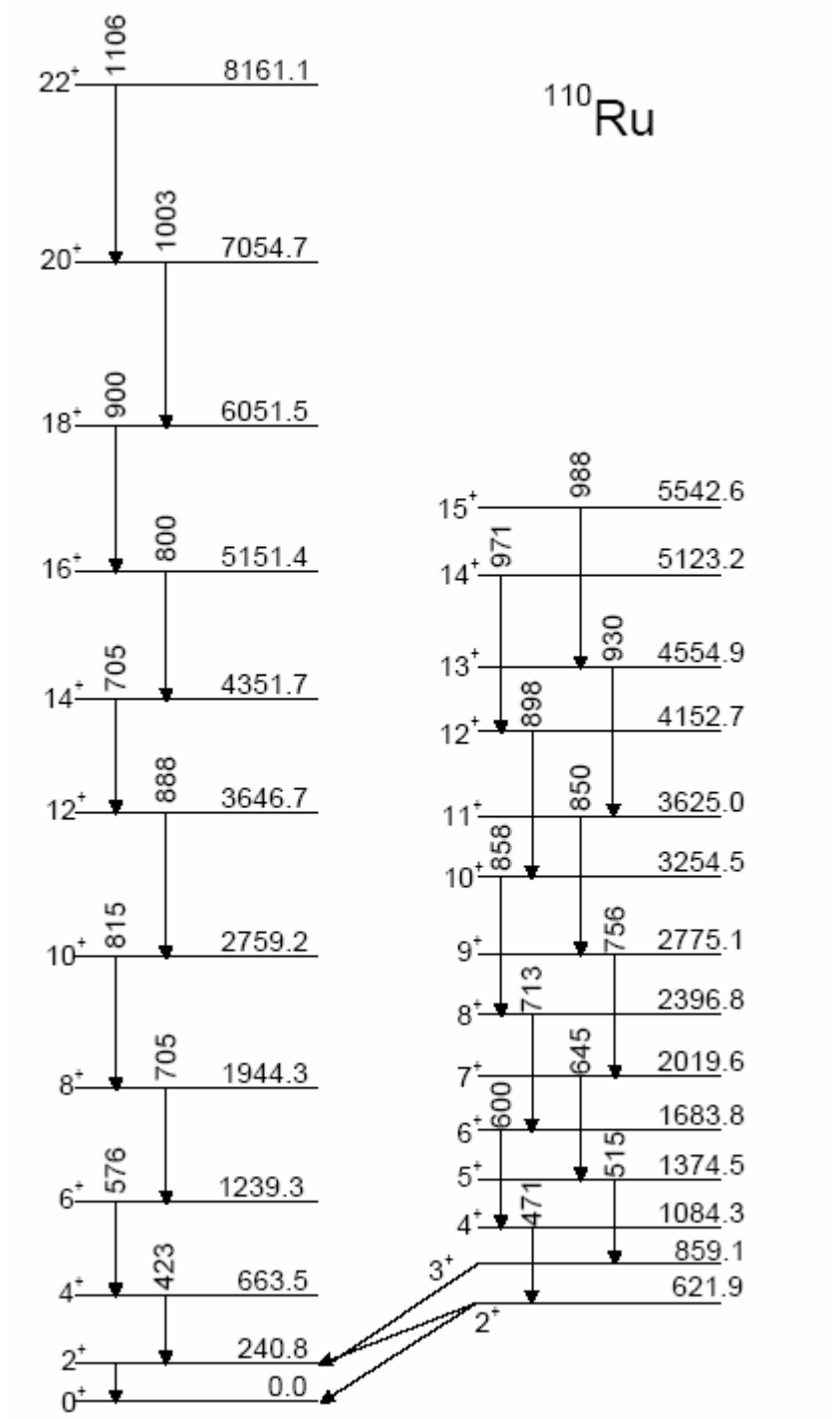

Figure 6. Partial level scheme of ^{110}Ru with energies labeled in keV. The uncertainty on the transition energies is ≈1 keV.

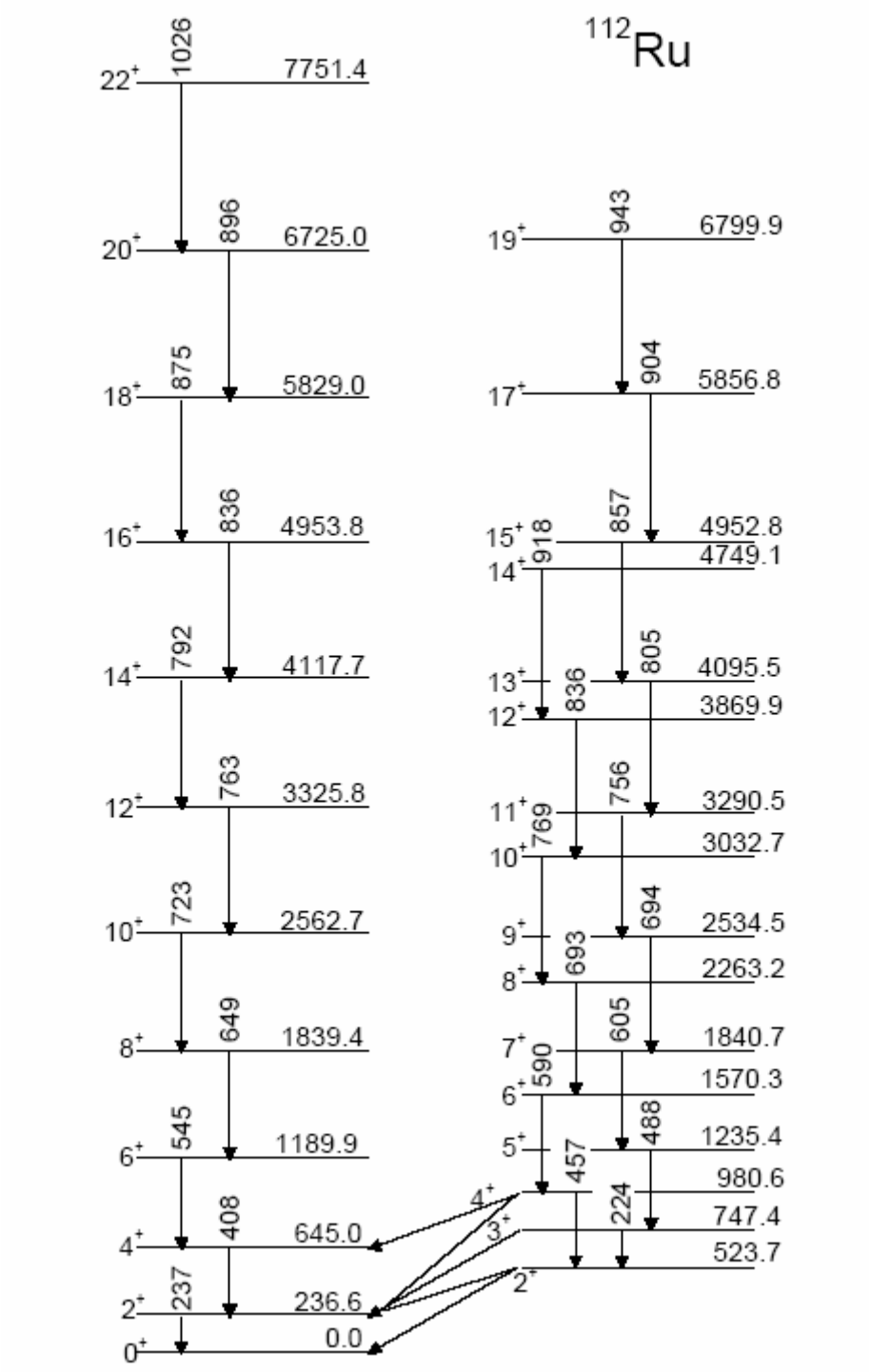

Figure 7. Partial level scheme of ^{112}Ru with energies labeled in keV. The uncertainty on the transition energies is ≈1 keV.

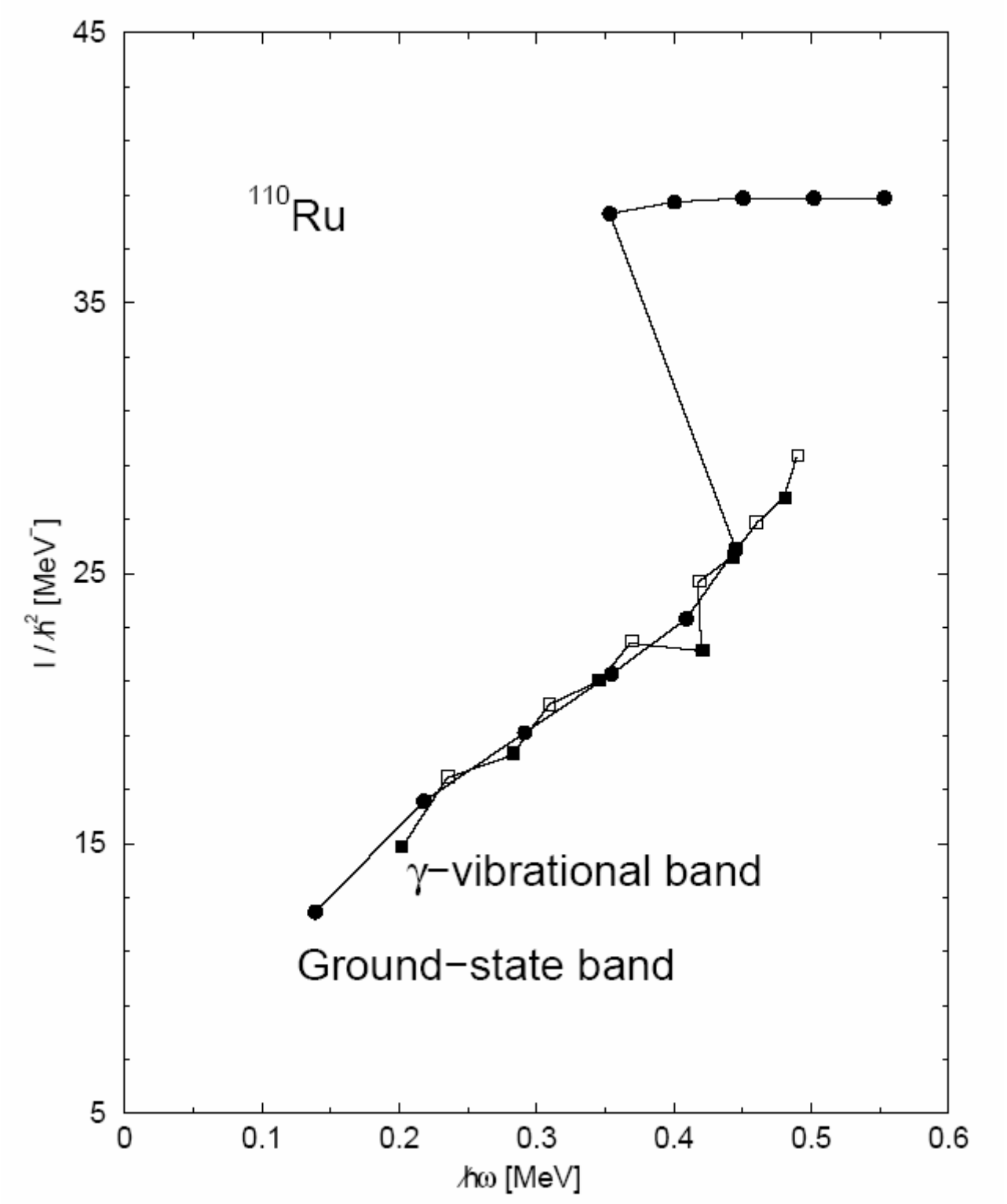

Figure 8. Kinematic moment of inertia as a function of rotational frequency for both ground-state band, labeled by filled circles, and γ-vibrational band, labeled by filled and open squares, in ^{110}Ru.

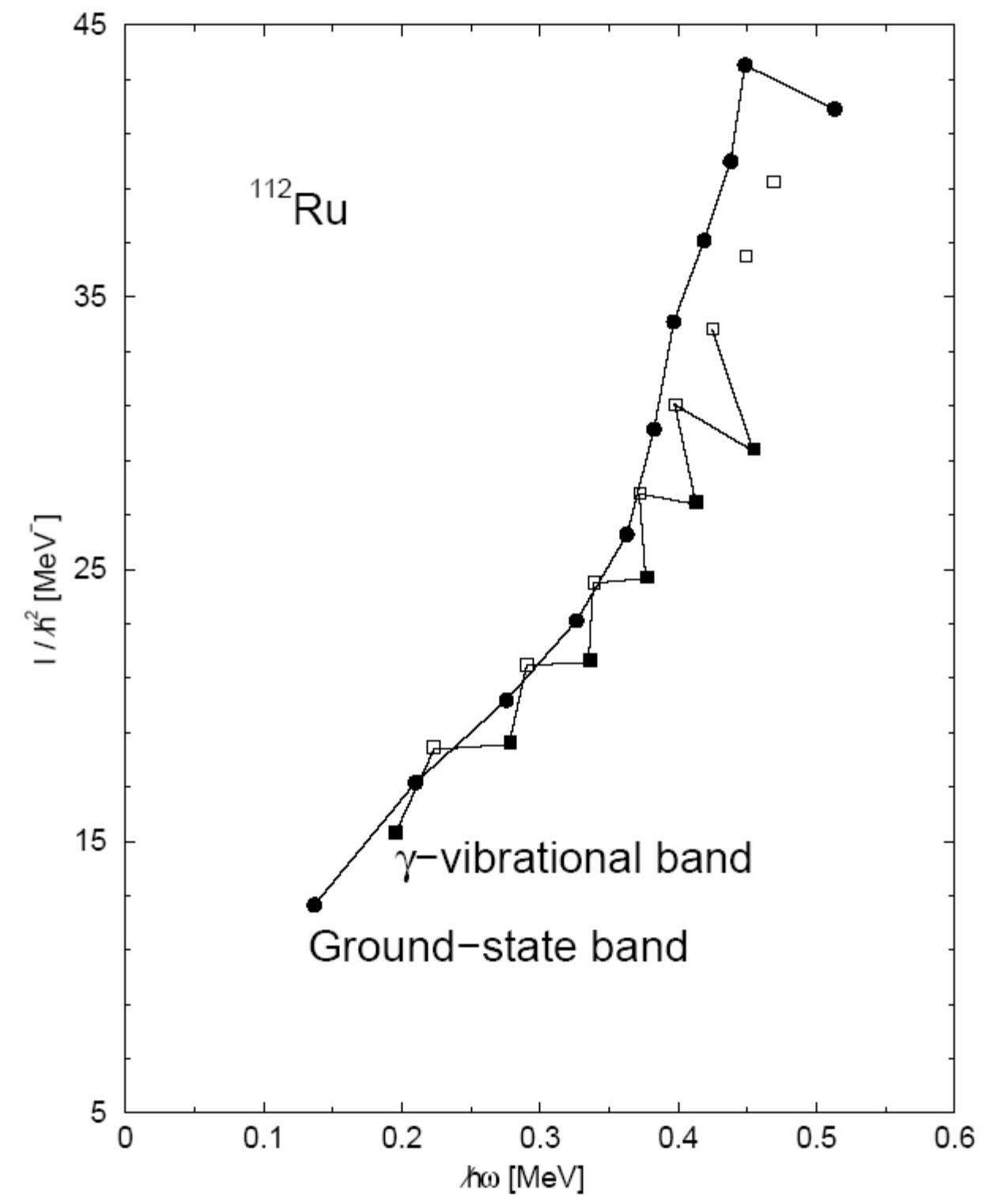

Figure 9. Kinematic moment of inertia as a function of rotational frequency for both ground-state band, labeled by filled circles, and γ-vibrational band, labeled by filled and open squares, in ^{112}Ru.

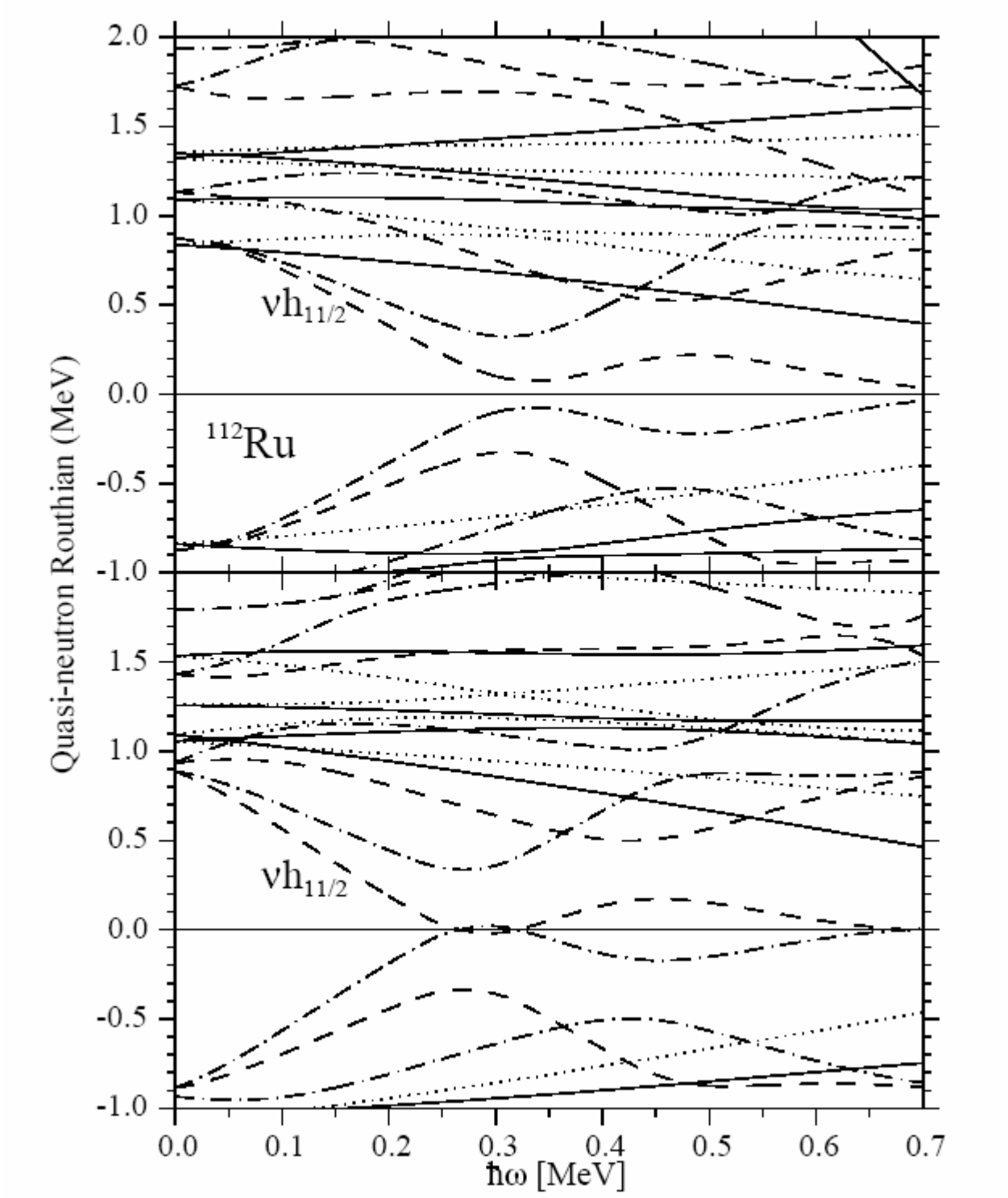

Figure 10. Cranked shell model calculations for quasineutrons in ^{112}Ru with β_2=0.29, β_4=0.0, and γ=−26^o (top) and −34^o (bottom). (π,α): solid=(+,+1/2), dotted=(+,−1/2), dash-dotted=(−,+1/2), dashed=(−,−1/2).

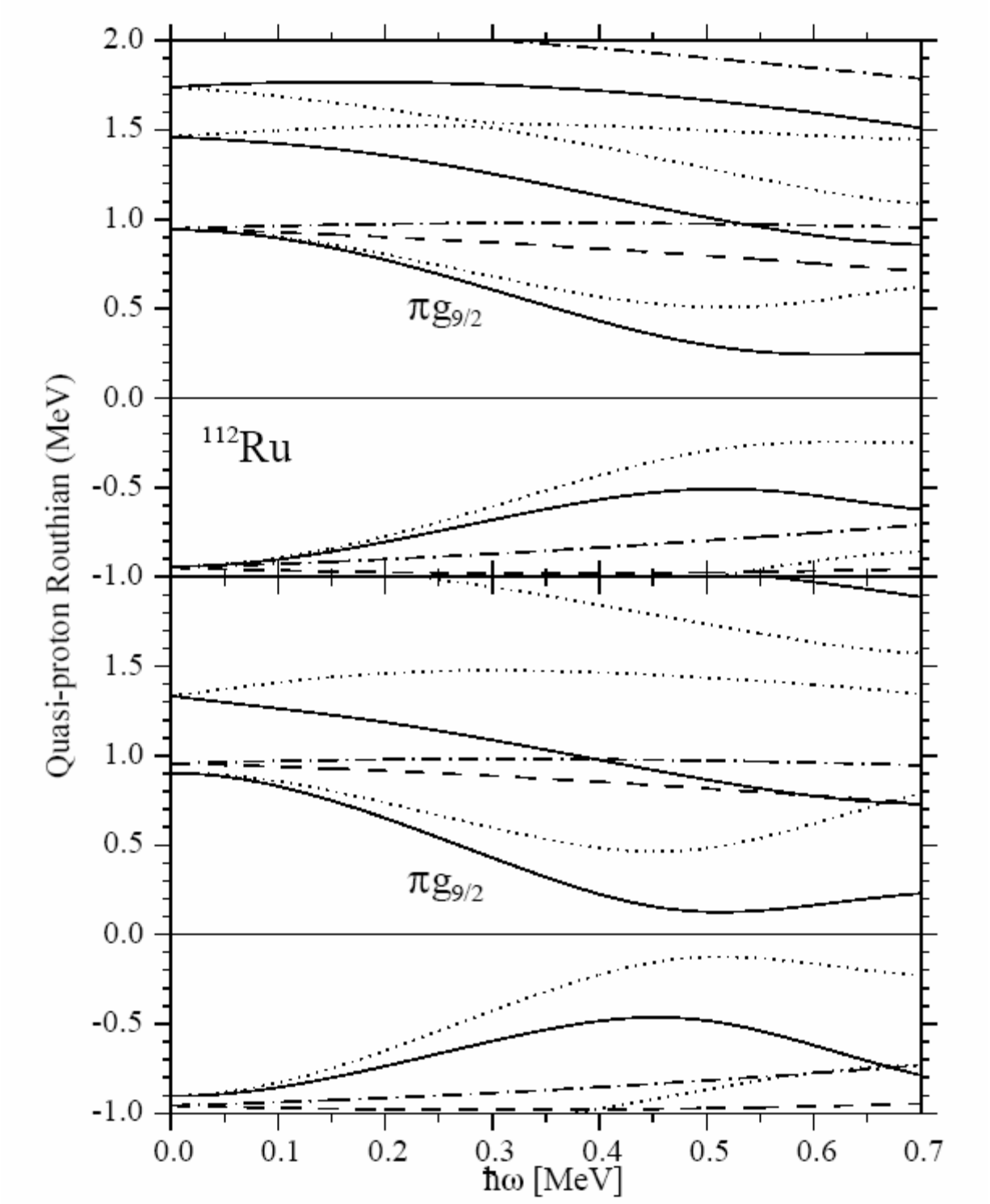

Figure 11. Cranked shell model calculations for quasiprotons in ^{112}Ru with β_2=0.29, β_4=0.0, and γ=−26^o (top) and −34^o (bottom). (π,α): solid=(+,+1/2), dotted=(+,−1/2), dash-dotted=(−,+1/2), dashed=(−,−1/2).